British Journal of Pharmacology (2005) 144, 595–604
www.nature.com/bjp

Effects of diltiazem and nifedipine on transient outward and ultra-rapid delayed rectifier potassium currents in human atrial myocytes

[1]Zhan Gao, [1]Haiying Sun, [2]Shui-Wah Chiu, [1]Chu-Pak Lau & *,[1]Gui-Rong Li

[1]Department of Medicine and Research Centre of Heart, Brain, Hormone and Health Aging, The University of Hong Kong, Pokfulam, Hong Kong SAR, China and [2]Cardiothoracic Unit, Faculty of Medicine, The University of Hong Kong, Pokfulam, Hong Kong SAR, China

1 It is unknown whether the widely used L-type Ca^{2+} channel antagonists diltiazem and nifedipine would block the repolarization K^+ currents, transient outward current (I_{to1}) and ultra-rapid delayed rectifier K^+ current (I_{Kur}), in human atrium. The present study was to determine the effects of diltiazem and nifedipine on I_{to1} and I_{Kur} in human atrial myocytes with whole-cell patch-clamp technique.

2 It was found that diltiazem substantially inhibited I_{to1} in a concentration-dependent manner, with an IC_{50} of $29.2 \pm 2.4\,\mu M$, and nifedipine showed a similar effect ($IC_{50} = 26.8 \pm 2.1\,\mu M$). The two drugs had no effect on voltage-dependent kinetics of the current; however, they accelerated I_{to1} inactivation significantly, suggesting an open channel block.

3 In addition, diltiazem and nifedipine suppressed I_{Kur} in a concentration-dependent manner (at $+50$ mV, $IC_{50} = 11.2 \pm 0.9$ and $8.2 \pm 0.8\,\mu M$, respectively). These results indicate that the Ca^{2+} channel blockers diltiazem and nifedipine substantially inhibit I_{to1} and I_{Kur} in human atrial myocytes.
British Journal of Pharmacology (2005) **144,** 595–604. doi:10.1038/sj.bjp.0706113
Published online 24 January 2005

Keywords: Human atrial myocyte; transient outward K^+ current; ultra-rapid delayed rectifier K^+ current; ion channels; diltiazem; nifedipine

Abbreviations: 4-AP, 4-aminopyridine; IC_{50}, the concentration for 50% maximum inhibition; $I_{Ca.L}$, L-type Ca^{2+} current; I_{Kur}, ultra-rapid delayed rectifier K^+ current; I_{to1}, transient outward K^+ current

Introduction

The 4-aminopyridine (4-AP)-sensitive transient outward K^+ current (I_{to1}) and ultra-rapid delayed rectifier K^+ current (I_{Kur}) play important roles in human atrial repolarization (Shibata *et al*., 1989; Wang *et al*., 1993; Li *et al*., 1995; 1996a). Inhibition of I_{to1} and/or I_{Kur} has been found to prolong the action potential duration in human atrium (Courtemanche *et al*., 1998; 1999; Van Wagoner, 2000). In addition, I_{Kur} has been reported to be present in the atrium, but not the ventricle of human heart (Li *et al*., 1996b). Therefore, blockade of I_{Kur} may be useful in the treatment of patients with atrial fibrillation, but without the risk of ventricular proarrhythmia (Van Wagoner, 2000; Van Wagoner & Nerbonne, 2000; Nattel, 2002).

The benzothiazopine Ca^{2+} channel blocker diltiazem and the dihydropyridine (DHP) Ca^{2+} channel blocker nifedipine are widely used in clinic for the treatment of cardiovascular diseases including hypertension (De Leeuw & Birkenhager, 2002; White, 2003), cardiac angina (Kumar & Hall, 2003), and/or supraventricular arrhythmias (for diltiazem) (Hohnloser *et al*., 2000). The therapeutic effects are generally believed to be related to the L-type Ca^{2+} channel ($I_{Ca.L}$) block (Hohnloser *et al*., 2000; De Leeuw & Birkenhager, 2001; Kumar & Hall, 2003; White, 2003). Earlier studies demonstrated that nifedipine significantly inhibited I_{to1} in rabbit atrial (Gotoh *et al*., 1991) and rat ventricular (Jahnel *et al*., 1994) cells. Our recent study found that the phenylalkylamine Ca^{2+} channel blocker verapamil substantially blocked I_{Kur}, but not I_{to1} in human atrial myocytes (Gao *et al*., 2004). Nevertheless, it is unknown whether diltiazem and nifedipine would affect human atrial repolarization currents. The present study was therefore designed to determine the effects of diltiazem and nifedipine on I_{to1} and I_{Kur} in human atrial myocytes with whole-cell patch-clamp technique.

*Author for correspondence at: Faculty of Medicine Building, The University of Hong Kong, L4-55, Laboratory Block, 21 Sassoon Road, Pokfulam, Hong Kong SAR, China;
E-mail: grli@hkucc.hku.hk
Published online 24 January 2005

Methods

Single atrial myocyte preparation

Atrial cells were isolated from specimens of human right atrial appendage obtained from 29 patients (57.7 ± 2.7 years old) undergoing coronary artery bypass grafting. The procedure for obtaining the tissues was approved by the Ethics Committee of the University of Hong Kong based on the patients' consent. All patients were free from supraventricular tachyarrhythmias, and the atria were grossly normal at the time of surgery. After excision, the samples were quickly immersed in oxygenated, nominally Ca^{2+}-free cardioplegic solution for transport to the laboratory. Atrial myocytes were enzymatically dissociated as

described previously (Du *et al*., 2003; Gao *et al*., 2004). Briefly, the myocardial tissue was sliced with a sharp blade, placed in a 15-ml centrifuge tube containing 10 ml of the Ca^{2+}-free Tyrode solution (36°C), and gently agitated by continuous bubbling with 100% O_2 for 15 min (5 min at a time in fresh solutions). The chunks were then incubated for 50 min in a similar solution containing 150–200 U ml^{-1} collagenase (CLS II, Worthington Biochemical, Freehold, NJ, U.S.A.), 0.2 mg ml^{-1} protease (type XXIV, Sigma Chemical, St Louis, MO, U.S.A.) and 1 mg ml^{-1} bovine serum albumin (Sigma). Subsequently, the supernatant was discarded. The chunks were re-incubated in a fresh enzyme solution with the same composition but no protease, microscope examination of the medium was performed every 10–15 min to determine the number and the quality of the isolated cells. When the yield appeared to be maximal, the chunks were suspended in a high K^+ medium containing (mM) 10 KCl, 120 K-glutamate, 10 KH_2PO_4, 1.8 $MgSO_4$, 10 taurine, 10 HEPES, 0.5 EGTA, 20 glucose, 10 mannitol, pH was adjusted to 7.3 with KOH and gently blown with a pipette. The isolated myocytes were kept at room temperature in the medium at least 1 h before use.

A small aliquot of the solution containing the isolated cells was placed in an open perfusion chamber (1-ml) mounted on the stage of an inverted microscope. Myocytes were allowed to adhere to the bottom of the chamber for 5–10 min and were then superfused at 2–3 ml min^{-1} with Tyrode solution. Only quiescent rod-shaped cells with clear cross-striations were used. The study was conducted at room temperature (21–22°C).

Solution and drugs

Ca^{2+}-free cardioplegic solution for specimen transport contained (in mM) 50 KH_2PO_4, 8 $MgSO_4$, 5 adenosine, 10 HEPES, 140 glucose, 100 mannitol, 10 taurine, pH was adjusted to 7.3. with KOH. Tyrode solution contained (in mM) 140 NaCl, 5.4 KCl, 1 $MgCl_2$, 1.0 $CaCl_2$, 0.33 NaH_2PO_4, 5 HEPES, 10 glucose, pH was adjusted to 7.4 with NaOH. The pipette solution contained (in mM) 20 KCl, 110 K-aspartate, 1.0 $MgCl_2$, 10 HEPES, 5 EGTA, 0.1 GTP, 5 Na_2-phosphocreatine, and 5 Mg_2-ATP, pH was adjusted to 7.2 with KOH. For I_{to1} and I_{Kur} recording, $BaCl_2$ (200 μM) and $CdCl_2$ (200 μM) were added to the superfusion to block I_{K1} and I_{Ca}. Atropine (1.0 μM) was used to minimize possible $I_{K,ACh}$ contamination during the current recording. Diltiazem was dissolved in distilled water with a stock solution of 100 mM, while a stock (100 mM) of nifedipine was made with DMSO. All the drugs were purchased from Sigma Chemicals Co. (St Louis, MO, U.S.A.).

Data acquisition and analysis

The whole-cell patch-clamp technique was used for electrophysiological recording. Borosilicate glass electrodes (1.2-mm OD) were pulled with a Brown-Flaming puller (model P-97, Sutter Instrument Co., Novato, CA, U.S.A.) and had tip resistances of 2–3 MΩ when filled with pipette solution. The whole-cell membrane currents in voltage-clamp mode were recorded using an EPC-9 amplifier and Pulse software (Heka, Lambrecht, Germany). A 3-M KCl-agar salt bridge was used as reference electrode. Liquid junction potentials were compensated before the pipette touched the cell. After a gigaseal was obtained, the cell membrane was ruptured by gentle suction to establish the whole-cell configuration. The cell membrane capacitance (78.6 ± 4.1 pF, $n = 46$) was directly measured using the lock-in module of the Pulse software, and used for normalizing the current in individual cells. The series resistance (R_s) was 3–8 MΩ and was compensated by 60–80% to minimize voltage errors. Current signals were low-pass filtered at 5 kHz and stored on the hard disk of an IBM compatible computer.

Nonlinear curve fitting was performed using Pulsefit (Heka) and/or Sigmaplot (SPSS Science, Chicago, IL, U.S.A.). Results are presented as mean ± s.e. Paired and/or unpaired Student's *t*-test was used as appropriate to evaluate the statistical significance of differences between two group means, and ANOVA was used for multiple groups. Values of $P < 0.05$ were considered statistical significant.

Results

Effect of diltiazem on I_{to1}

Figure 1A shows voltage-dependent I_{to1} elicited by 300-ms voltage steps to between −40 and +50 from −50 mV (as shown in the inset) at 0. 2 Hz in a representative human atrial myocyte during control, in the presence of diltiazem, and after the drug washout. I_{to1} was substantially inhibited by the application of 5 and 50 μM diltiazem, and the effect recovered after washout of the drug for 8 min. Figure 1B illustrates the time-dependent effect of diltiazem on I_{to1} activated by the voltage step shown in the left inset. The current measured was peak to 'quasi'-steady-state level. Diltiazem at 50 μM gradually inhibited I_{to1}, and the effect reached a steady-state level within 2 min. The current completely recovered upon the drug washout. The original I_{to1} traces at the corresponding time points are shown in the right inset of the panel.

Results from Figure 1 indicate that the sustained current (i.e. I_{Kur}) is also suppressed when I_{to1} is inhibited by diltiazem. It would be relatively accurate in evaluating the diltiazem effect on I_{to1} if a selective I_{Kur} inhibitor is available to separate I_{to1}. It was reported that 4-AP selectively inhibited I_{Kur} at low concentrations (50 μM, about 50% inhibition) (Wang *et al*., 1993; Li *et al*., 1996b), but higher concentrations of 4-AP (> 50 μM) also suppressed I_{to1} significantly (authors' unpublished observation). Therefore, 4-AP would not be an ideal compound to separate I_{to1}. We have recently found that verapamil inhibits I_{Kur} ($IC_{50} = 3.2$ μM) without reducing I_{to1} amplitude, while it induces an increase of measured I_{to1} in human atrial myocytes (Gao *et al*., 2004). Therefore, verapamil was used to separate I_{to1} as described in the following. We felt that the use of verapamil to limit the possible contamination of I_{Kur} would not affect drug action on I_{to1}.

Figure 2A displays representative recordings of I_{to1} elicited with the protocol as shown in the inset during control, in the presence of 10 μM verapamil, co-presence of verapamil and 50 μM diltiazem, and washout of diltiazem. After the inhibition of I_{Kur} by verapamil, inactivation of I_{to1} was actually increased, and the measured I_{to1} was clearly enhanced as the previous report observed (Gao *et al*., 2004). Diltiazem at 50 μM substantially suppressed I_{to1}, and the effect reversed upon dug washout. Figure 2B shows the *I–V* relationships of I_{to1} in seven cells during the pretreatment of 10 μM verapamil to

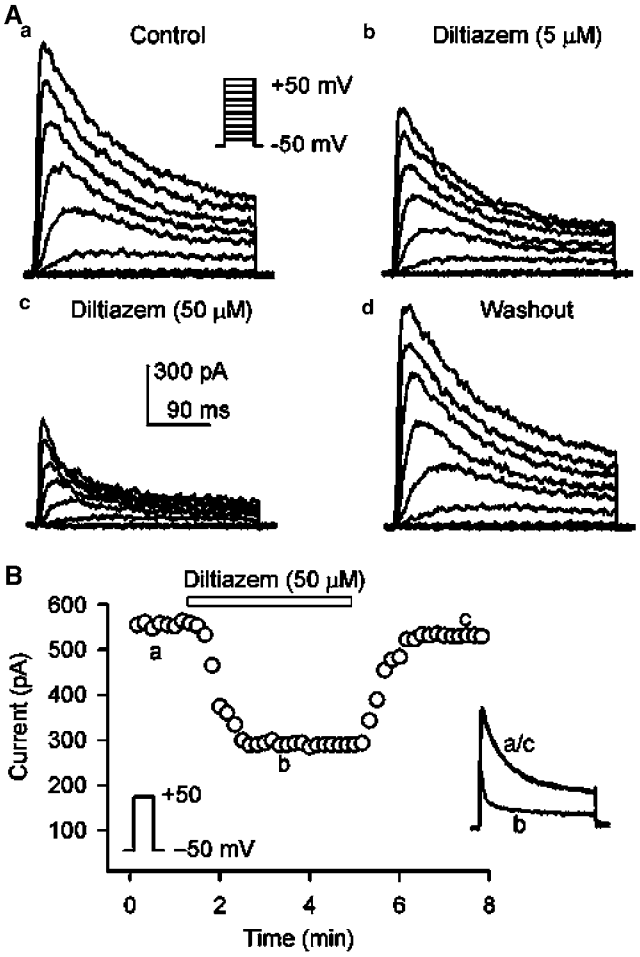

Figure 1 Diltiazem effect on I_{to1}. (A) Representative voltage-dependent I_{to1} (capacitance compensated) recorded in an atrial myocyte with the voltage steps protocol shown in the inset at 0.2 Hz under control conditions (a), in the presence of 5 and 50 μM diltiazem (b, c). I_{to1} was substantially inhibited by the application of diltiazem for 6 min, and the effect was recovered by the drug washout for 8 min (d). (B) Time-dependent effect of 50 μM diltiazem on I_{to1} elicited by the voltage step shown in the left inset delivered every 10 s in a typical experiment. I_{to1} measured was peak to 'quasi'-steady-state level. The original I_{to1} traces at corresponding time points are shown in the right inset of the panel.

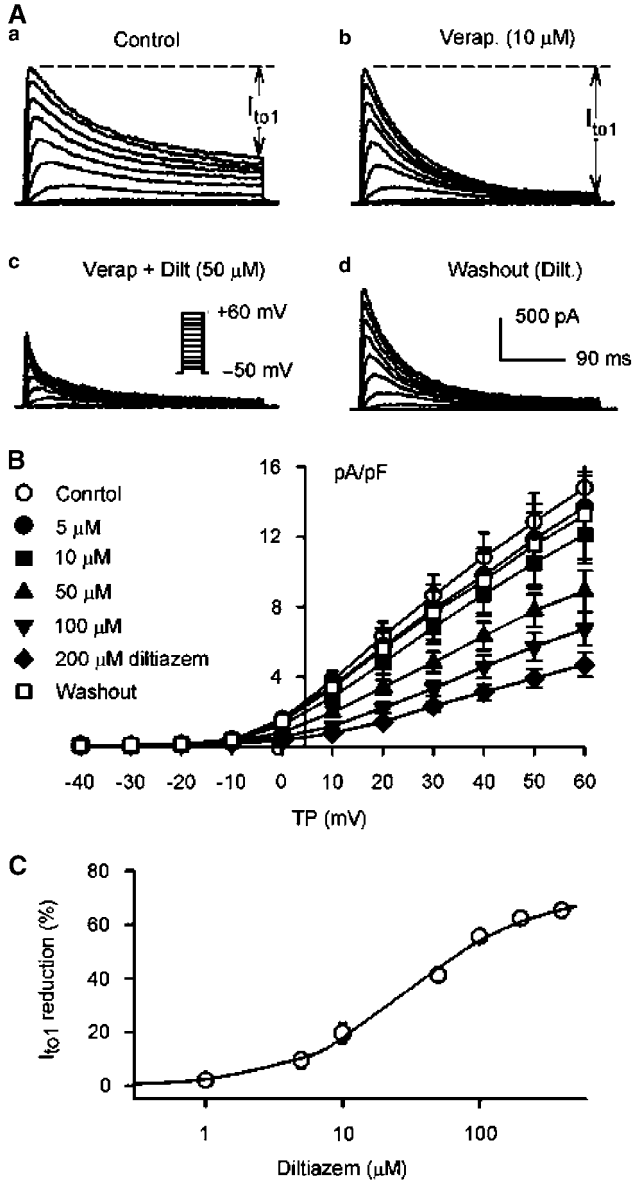

Figure 2 Effects of verapamil and diltiazem on I_{to1}. (A) I_{to1} traces recorded with the voltage protocol as shown in the inset of (c) in a representative myocytes during control (a), in the presence of 10 μM verapamil (Verap.) for 6 min (b), co-presence of verapamil and 50 μM diltiazem (Dilt.) for 6 min (c), and washout of diltiazem for 8 min. Verapamil actually induced an increase of measured I_{to1} by selectively inhibiting I_{Kur}. (B) *I–V* relationships of I_{to1} in the presence of 10 μM verapamil (control), co-presence of verapamil and 5, 10, 50, 100, and 200 μM diltiazem (6 min for each concentration), and after the drug washout for 10 min. Diltiazem inhibited I_{to1} in a concentration-dependent manner ($P<0.05$ or 0.01 vs control, and the effect was reversed by 90% after the drug washout. The statistical significance was analyzed by repeated-measures ANOVA. (C) Concentration–response relationship for diltiazem inhibition of I_{to1}. Symbols are mean data at +50 mV (the error bars are smaller than the size of the data symbol), and solid line is the best-fit Hill equation, $IC_{50}=29.2\pm2.4$ μM, Hill co-efficient $=0.98\pm0.08$ ($n=6$), and $E_{max}=65.2\%$.

inhibit I_{Kur}, and after the application of 5, 10, 50, 100, and 200 μM diltiazem, showing that diltiazem inhibits I_{to1} in a concentration-dependent manner. The effect was reversed by 90% after washout of diltiazem. Diltiazem at 5–200 μM significantly suppressed I_{to1} at voltages from 0 to +60 mV ($P<0.05$ or 0.01 vs control). Figure 2C illustrates the concentration–response relationship for the inhibition of I_{to1} by diltiazem. In six cells completed all the concentrations from 1 to 400 μM, data were fit to the Hill equation: $E=E_{max}/[1+(IC_{50}/C)^b]$, where E is the effect at concentration C, E_{max} is the maximal effect, IC_{50} is the concentration for half-maximal effect, and b is Hill coefficient. IC_{50} (at +50 mV) was 29.2 ± 2.4 μM with a Hill co-efficient of 0.97 ± 0.06 on the basis of cell-by-cell fits, and E_{max} was 65.2%.

Time-dependent kinetics of I_{to1} were determined in the presence of 10 μM verapamil. Figure 3a shows current traces (points) upon a 300-ms voltage step to +50 from –50 mV in a representative cell in the presence of 10 μM verapamil (control), and co-presence of verapamil and 50 μM diltiazem. I_{to1} was well fitted by a mono-exponential function (solid line) under control conditions with time constant shown. After the

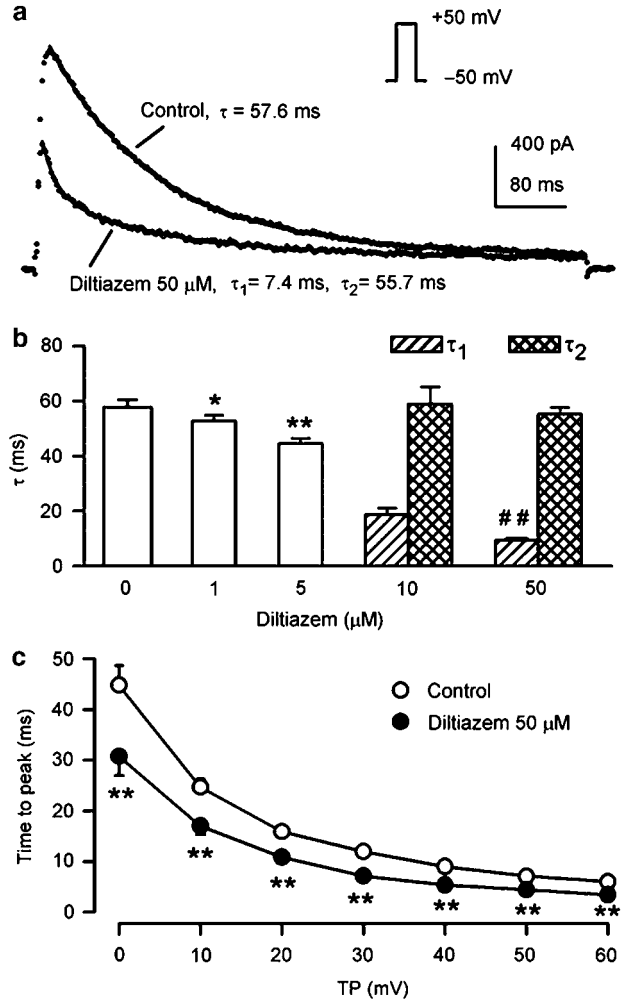

Figure 3 Effects of diltiazem on time-dependent kinetics of I_{to1}. (a) I_{to1} traces recorded from a representative cell upon a 300-ms voltage step to +50 from −50 mV in the presence of 10 μM verapamil (control) and co-presence of verapamil and 50 μM diltiazem. Raw data (points) of I_{to1} under control conditions were fitted to a monoexponential function (solid lines, superimposed with raw data) with time constants shown. After the application of 50 μM diltiazem, the data were fitted only by a biexponential equation, with fast and slow time constants (τ_1 and τ_2) shown. (b) Mean values of time constants at +50 mV under control conditions, in the presence of 1, 5, 10, and 50 μM diltiazem. The time constant was reduced by the application of 1 and 5 μM diltiazem ($n=7$, $^*P<0.05$, $^{**}P<0.01$ vs control). Diltiazem at concentrations higher than 10 μM had τ_1 and τ_2. The τ_1 decreased with increasing diltiazem concentration ($^{\#\#}P<0.01$ vs 10 μM diltiazem), and the τ_2 did not show significant difference. (c) Time to peak of I_{to1} activation at 0 to +60 mV under control conditions and in the presence of 50 μM diltiazem. Diltiazem significantly reduced the time to peak of I_{to1} ($n=7$, $^{**}P<0.01$ vs control). The statistical significance was analyzed by repeated-measures ANOVA.

application of 50 μM diltiazem, the current trace was no longer fitted by the monoexponential function, but well fitted by a biexponential equation with the time constants (τ_1 and τ_2) shown. A similar finding was obtained in all of the experiments in the presence of 10 and 50 μM diltiazem. Figure 3b illustrates the averaged time constants. The time constant of I_{to1} inactivation was reduced from 57.8±2.8 ms of control to 52.1±2.1 and 44.1±1.8 ms respectively ($P<0.05$ or 0.01 vs control) by the application of 1 and 5 μM diltiazem. At 10 and 50 μM, there was a slower component with a time constant (τ_2) similar to that under control conditions, and a faster component whose time constant (τ_1) decreased to 9.4±0.6 ms from 18.6±2.1 ms as the drug concentration increased ($n=7$, $P<0.01$). These results are consistent with high-affinity open-channel block causing rapid current decay. Figure 3c shows the time to peak of I_{to1}, determined from the onset of depolarization to the current peak. Diltiazem at 50 μM significantly reduced the time to peak of I_{to1} at 0 to +60 mV ($n=6$, $P<0.01$ vs control), consistent with open-channel block action (Feng *et al.*, 1997).

Voltage dependence of I_{to1} activation and inactivation was evaluated in the presence of 10 μM verapamil (control), and co-presence of verapamil and 50 μM diltiazem. The variable (g) of voltage-dependent activation was calculated from I–V relationships for each cell from Figure 2B, based on the formulation $g=I/(V_t-V_r)$ as described previously (Du *et al.*, 2003), where I is the peak current at the test voltage (V_t), and V_r is the measured reversal potential (~70 mV). The variable

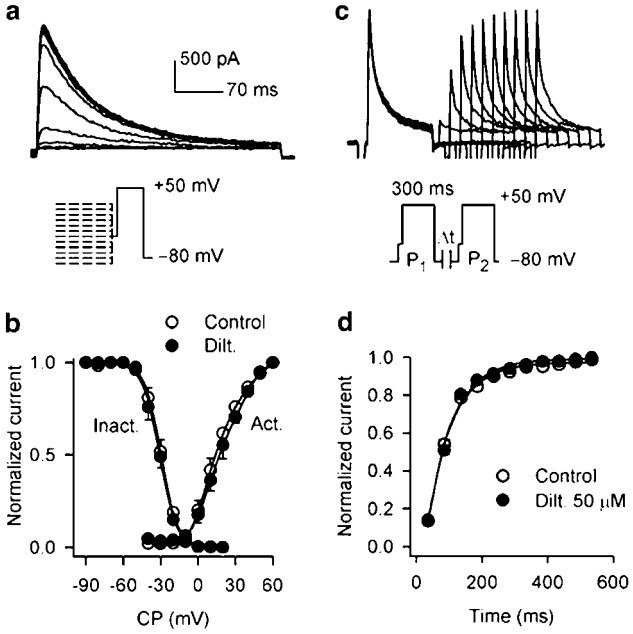

Figure 4 Effects of diltiazem on voltage-dependence and restoration of I_{to1}. (a) Representative current traces and protocol (inset) used to evaluate voltage-dependent inactivation I_{to1} recorded in the presence of 10 μM verapamil. (b) Voltage-dependent variables for I_{to1} activation (Act.) and inactivation (Inact.) were fitted to the Boltzmann distribution: $y=1/\{1+\exp[(V_m-V_{0.5})/S]\}$, where V_m is membrane potential, $V_{0.5}$ is the midpoint, and S is slope. For activation, $V_{0.5}$ and S were 16.9±1.4 and −11.2±0.3 mV for control, and 18.4±0.9 and −11.9±0.4 mV for 50 μM diltiazem (Dilt.) treatment ($n=7$, $P=$NS). For inactivation, $V_{0.5}$ and S were −29.2±1.1 and 7.5±0.6 mV under control conditions, and −30.4±1.4 and 7.6±0.8 mV in the presence of 50 μM diltiazem ($n=6$, $P=$NS). (c) Representative current traces recorded in a typical experiment in the presence of 10 μM verapamil by 300-ms paired pulses to +50 mV after a 30-ms step of −40 mV (to inactivate I_{Na}) from −80 mV with varying P1 and P2 interval (inset), which are used for assessing time-dependent recovery of I_{to1} from inactivation. (d) Mean data for time course of recovery of I_{to1} from inactivation in the absence and presence of 50 μM diltiazem in six cells. Data were best fit to monoexponential function. No change in recovery time constant of I_{to1} was observed after the application of diltiazem ($n=6$, $P=$NS).

(I/I_{max}) for voltage-dependent inactivation was determined with a protocol as illustrated in Figure 4a, with 1−s conditioning pulses from voltages between −90 and +20 mV, followed by a 300-ms test pulse to +50 mV after a 30-ms interval at −40 mV. Mean data for activation and inactivation, along with best-fit Boltzmann equation to obtain the half activation or inactivation voltage ($V_{0.5}$) and the slope (S), under control conditions and in the presence of 50 μM diltiazem are shown in Figure 4b. The voltage dependence of I_{to1} activation and inactivation was not affected by the application of diltiazem. $V_{0.5}$ and S were 16.9±1.4 and −11.2±0.3 mV for activation, and −29.2±1.1 and 7.5±0.6 mV for inactivation under control conditions. In the presence of 50 μM diltiazem, the corresponding values were 18.4±0.9 and −11.9±0.4 mV for activation ($n=7$, $P=$NS), and –30.4±1.4 and 7.6±0.8 mV for inactivation ($n=6$, $P=$NS).

Time-dependent recovery of I_{to1} from inactivation was studied with a paired-pulse protocol as shown in the inset of Figure 4c. Time course of recovery was well fitted by a monoexponential function with the time constant of 98.6±5.4 ms under control conditions, and 105.8±7.5 ms in the presence of 50 μM diltiazem ($n=6$, $P=$NS). The result indicates that diltiazem does not affect recovery of I_{to1} from inactivation. In addition, no use-dependent effect of diltiazem (50 μM) on I_{to1} (+50 mV) was noted at frequencies from 1 to 3 Hz ($n=5$, $P=$NS).

Inhibition of I_{Kur} *by diltiazem*

As described previously (Wang *et al*., 1993; Li *et al*., 1996a; Du *et al*., 2003; Gao *et al*., 2004), I_{Kur} was recorded with a 100-ms prepulse to +40 mV to partially inactivate I_{to1}, followed by 150-ms test pulses to between −40 and +50 from −50 mV after a 10-ms interval, then to −30 mV (as shown in the inset in Figure 5A). Figure 5A displays voltage-dependent I_{Kur} recorded by the voltage protocol in a typical experiment. Under control conditions the current was rapidly activated by depolarization steps with significant tail current at –30 mV. Diltiazem at 5 and 50 μM substantially inhibited both I_{Kur} and tail current. The effect was significantly recovered by the drug washout. Figure 5B shows the time-dependent effect of 10 μM diltiazem on I_{Kur} activated by the voltage protocol shown in the left inset in a representative myocyte. I_{Kur} measured from zero level to the current at the end of voltage step. I_{Kur} was gradually inhibited by diltiazem, and recovered upon the drug washout. The original I_{Kur} traces at corresponding time points are shown in the right inset of the panel.

Figure 6a displays the I–V relationships of I_{Kur} ($n=8$) under control conditions, in the presence of 1, 5, 10, 50, and 100 μM diltiazem, and after washout of the drug, showing that diltiazem blocks I_{Kur} in a concentration-dependent manner. Figure 6b summarizes the percent reduction of I_{Kur} by diltiazem at voltages from 0 to +50 mV. Significant inhibitory effect of I_{Kur} by diltiazem was observed from the low concentration of 1 μM. At concentrations from 10 to 100 μM, diltiazem showed voltage-dependent effect on I_{Kur}, and the inhibition was stronger at voltages positive to +10 mV ($P<0.05$ or 0.01 vs 0 mV). Figure 6c shows the concentration–response relationships for suppression of I_{Kur} at +50 mV by diltiazem in seven cells completed all the concentrations from 0.1 to 200 μM. Mean IC_{50} was 11.2±0.9 μM with a Hill co-efficient of 0.96±0.07, and E_{max} was 64%. No use-dependent inhibition of I_{Kur} (+40 mV) by diltiazem (10 μM) was observed at frequencies from 1 to 3 Hz ($n=6$, $P=$NS).

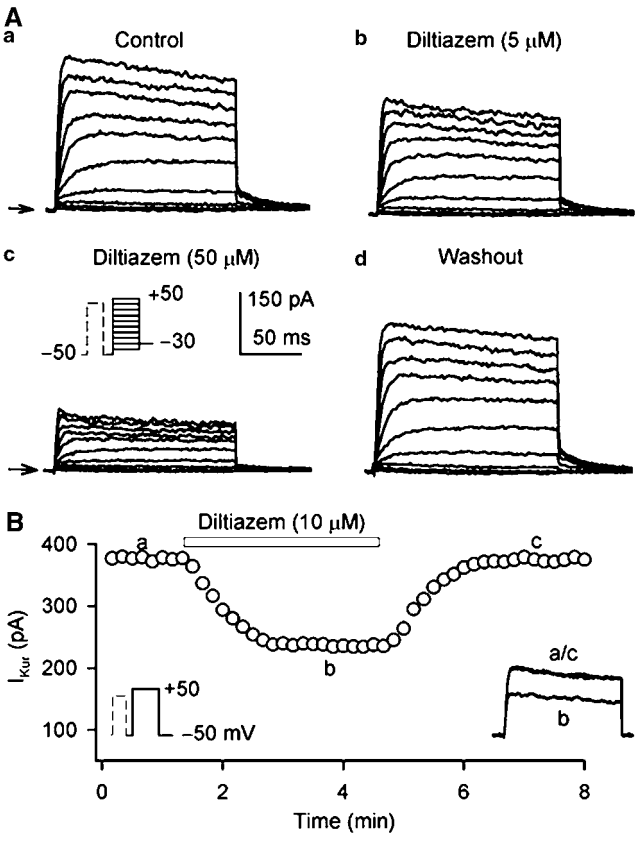

Figure 5 Effect of diltiazem on I_{Kur}. (A) Representative voltage-dependent I_{Kur} (capacitance compensated) recorded at 0.2 Hz in a typical experiment with a 100-ms prepulse to +40 mV to inactivate I_{to1}, followed by 150-ms test pulses to between –40 and +50 from –50 mV after a 10-ms interval, then to –30 mV (as shown in the inset of (c) under control conditions (a), in the presence of 5 and 50 μM diltiazem (b, c). I_{Kur} was substantially suppressed by the application of diltiazem, and the effect was significantly recovered by washout of the drug for 6 min (d). (B) Time-dependent effect of 10 μM diltiazem on I_{Kur} elicited by 150-ms voltage step to +50 from −50 mV (as shown in the left inset) delivered every 10 s. The original I_{Kur} races at corresponding time points are shown in the right inset.

Nifedipine effect on I_{to1}

Figure 7A shows the time-dependent effect of nifedipine on I_{to1} activated by a 300-ms voltage to +50 from –50 mV (as shown in the left inset) in a human atrial myocyte. Nifedipine gradually inhibited I_{to1}, and the effect recovered upon the drug washout. Figure 7B displays voltage-dependent I_{to1} recorded with the voltage protocol as shown in the inset in a representative cell under control conditions, and after the application of nifedipine. Nifedipine at 5 and 50 μM substantially suppressed I_{to1}, and accelerated the inactivation of the current. These effects reversed upon drug washout.

As diltiazem did, nifedipine suppressed both I_{to1} and I_{Kur}. Verapamil at 10 μM was therefore used to inhibit I_{Kur} to obtain a relatively accurate effect of nifedipine on I_{to1}. Figure 8A displays representative recordings of I_{to1} in the presence of

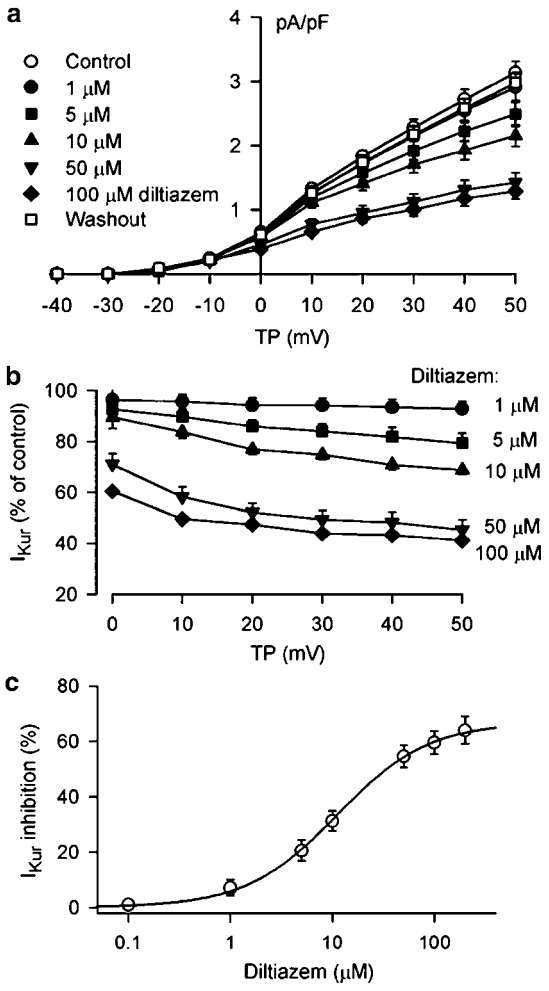

Figure 6 Concentration-dependent effect of diltiazem on I_{Kur}. (a) *I–V* relationships of I_{Kur} under control conditions, in the presence of 1, 5, 10, 50, and 100 μM diltiazem (6 min for each concentration), and after the drug washout for 10 min. Diltiazem inhibited I_{Kur} in a concentration-dependent manner, and the effect was reversed by 95% (at +50 mV) after the drug washout. (b) Percent reduction of I_{Kur} at 0 to +50 mV by diltiazem with multiple concentrations. Diltiazem significantly inhibited I_{Kur} at concentrations from 1 μM ($P<0.05$ vs control) to 5, 10, 50, and 100 μM ($n=8$, $P<0.01$ vs control). Significant voltage dependence was observed for the drug effect at 10–100 μM, and stronger effect was observed at potentials positive to +10 and +50 mV ($P<0.05$ or 0.01 vs 0 mV). The statistical significance was analyzed by repeated-measures ANOVA. (c) Concentration–response relationships of I_{Kur} block by diltiazem at +50 mV. The symbols are mean values of inhibitory effect in cells exposed to different concentrations (0.1–200 μM) of diltiazem. Solid lines were best fit to Hill equation. Mean IC_{50} was 11.2 ± 0.9 μM, Hill co-efficient was 0.96 ± 0.07, and E_{max} was 64% ($n=7$).

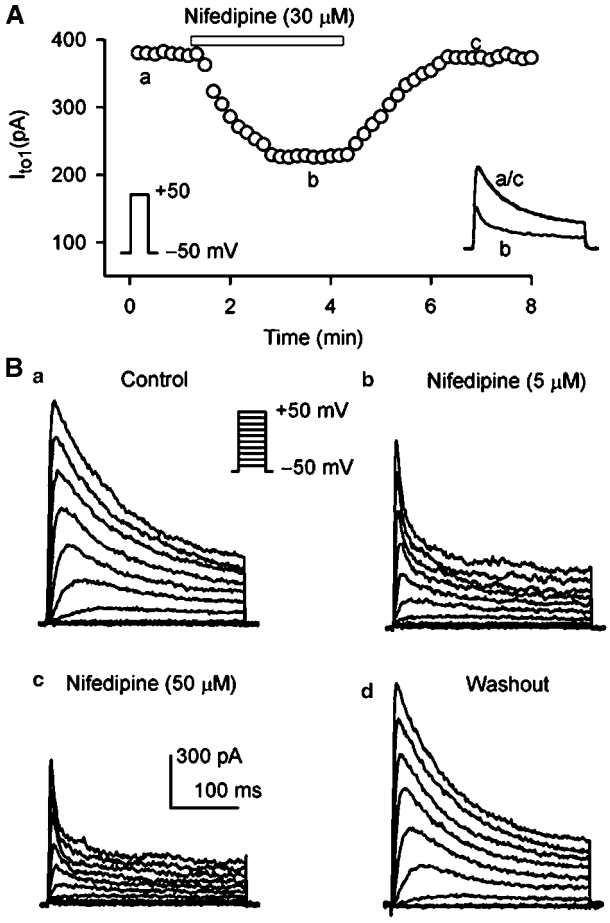

Figure 7 Inhibition of I_{to1} by nifedipine. (A) Time-dependent effect of 30 μM nifedipine on I_{to1} elicited by voltage step to +50 from −50 mV (as shown in the left inset) delivered every 10 s. Nifedipine reversibly suppressed I_{to1}. The original I_{to1} traces at corresponding time points are shown in the right inset. (B) Voltage-dependent I_{to1} traces recorded with the voltage protocol as shown in the inset in a typical experiment under control conditions (a), in the presence of 5 and 50 μM nifedipine (b, c) for 5 min. I_{to1} was significantly inhibited by nifedipine, and the effect recovered upon the drug washout for 6 min.

10 μM verapamil (control), co-presence of verapamil and 5 and 50 μM nifedipine, and washout of nifedipine. Figure 8B illustrates the *I–V* relationships of I_{to1} in seven cells before and after the application of 5, 10, 50, and 100 μM. I_{to1} was suppressed by nifedipine in a concentration-dependent manner, and recovered by 80.1% upon washout of nifedipine. Nifedipine significantly inhibited I_{to1} at voltages from 0 to +60 mV ($P<0.05$ or $P<0.01$ vs control) with 5, 10, 50, and 100 μM nifedipine. The concentration–response relationship for inhibition of I_{to1} by nifedipine is illustrated in Figure 8C. On the basis of cell-by-cell fits with the Hill equation in six cells, IC_{50} was 26.8 ± 2.1 μM with a Hill co-efficient of 0.96 ± 0.05 ($n=6$), and E_{max} was 85.1%.

Effects of nifedipine on time-dependent inactivation of I_{to1} were determined under conditions of I_{Kur} inhibition by 10 μM verapamil. Figure 9a displays the representative I_{to1} traces (points) upon a 300-ms voltage step to +50 from −50 mV, well fitted by a monoexponential function (solid line) under control conditions, but only best fitted by a biexponential function after the application of 50 μM nifedipine with fast and slow time constants (τ_1 and τ_2) shown. Figure 9b summarizes mean values of the time constants studied in seven cells under control conditions, and after the application of 1, 5, 10, and 50 μM nifedipine. In the presence of 1 μM nifedipine, the monoexponential time constant reduced to 39.4 ± 3.7 from 45.2 ± 4.2 ms of control ($n=7$, $P<0.05$). At higher concentrations of nifedipine at 5, 10, and 50 μM, there was a slower component with a time constant (τ_2) similar to that under control conditions, and a faster component whose time constant (τ_1)

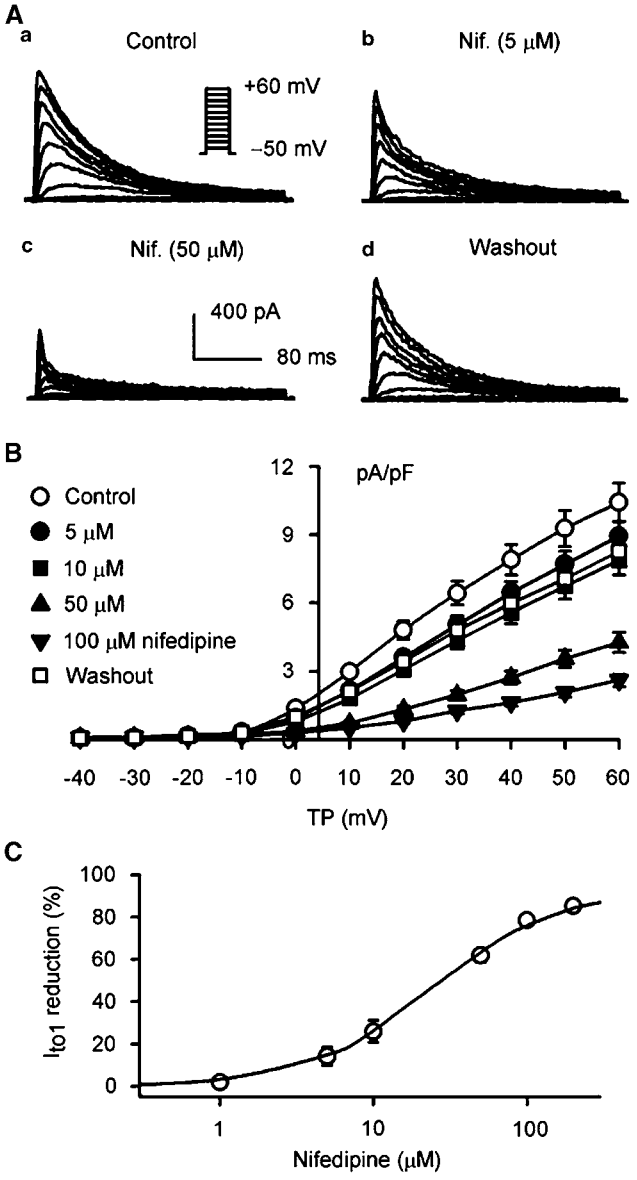

Figure 8 Effect of nifedipine on I_{to1} under conditions of inhibiting I_{Kur} with 10 μM verapamil. (A) I_{to1} traces recorded with the same voltage protocol as shown in the inset in a representative myocyte during control (a, 10 μM verapamil), in the co-presence of verapamil and 5 (b) and 50 (c) μM nifedipine (Nif.) for 6 min, and washout of nifedipine for 10 min (d). (B) *I–V* relationships of I_{to1} under control conditions (10 μM verapamil), in the co-presence of verapamil and 5, 10, 50, 100 μM nifedipine (6 min for each concentration), and after the drug washout for 10 min. Nifedipine (5–100 μM) significantly inhibited I_{to1} at voltages from 0 to +60 mV ($n=7$, $P<0.05$ or 0.01). The statistical significance was analyzed by repeated-measures ANOVA. (C) Concentration-dependent response of I_{to1} to nifedipine. IC_{50} at +50 mV was 26.8±2.1 μM with a Hill co-efficient of 0.97±0.02 ($n=6$), and E_{max} was 85.1%.

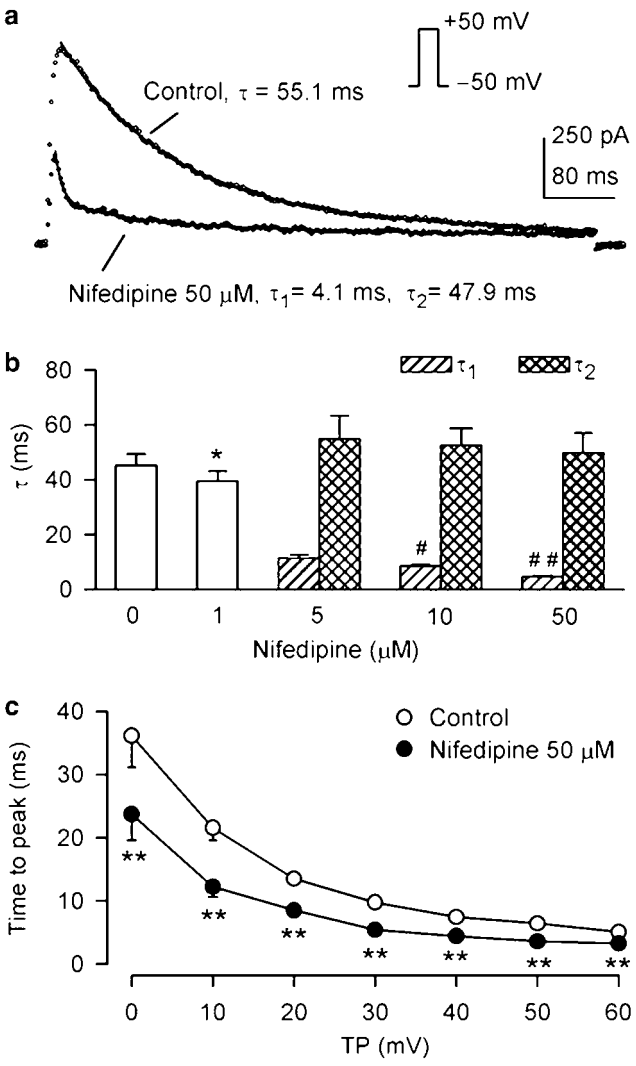

Figure 9 Effects of nifedipine on inactivation and time to peak of I_{to1}. (a) I_{to1} traces recorded in a typical experiment upon a 300-ms voltage step to +50 from −50 mV in the presence of 10 μM verapamil (control), and co-presence of verapamil and 50 μM nifedipine. Raw data (points) of I_{to1} under control conditions were well fit to a mono-exponential function (solid lines, superimposed with raw data) with time constant shown. The data after application of 50 μM nifedipine were only fit to a biexponential equation with fast and slow time constants (τ_1 and τ_2) shown. (b) Mean values of I_{to1} inactivation time constants under control conditions, and in the presence of 1 ($n=7$, $P<0.05$ vs control), 5, 10 and 50 μM nifedipine ($^{\#}P<0.05$, $^{\#\#}P<0.01$ vs 5 μM nifedipine). (c) Time to peak of I_{to1} as a function of test potentials under control conditions and in the presence of 50 μM nifedipine. The time to peak of I_{to1} was significantly reduced at 0 to +60 mV by the application of diltiazem ($n=6$, $^{**}P<0.01$ vs control). The statistical significance was analyzed by repeated-measures ANOVA.

decreased with increasing nifedipine concentration ($P<0.01$). Figure 9c illustrates mean values of the time to peak of the onset of I_{to1} activation before and after the employment of 50 μM nifedipine, showing that nifedipine significantly reduces the time to peak of I_{to1} at 0 to +60 mV ($n=6$, $P<0.01$ vs control). These results suggest that nifedipine inhibits I_{to1} *via* open channel block.

No change in voltage-dependent and recovery kinetics of I_{to1} was observed with 50 μM nifedipine. $V_{0.5}$'s of voltage-dependent activation and inactivation of I_{to1} were 16.4±2.1 and −28.1±2.4 mV under control conditions, and 18.7±2.8 ($n=7$) and −31.5±2.9 mV ($n=6$) after the application of 50 μM nifedipine ($P=$NS). The time constant (τ) of recovery of I_{to1} from inactivation was 97.3±4.9 ms under control conditions, and 89.5±6.2 ms in the presence of 50 μM nifedipine ($n=6$, $P=$NS vs control). No use-dependent effect of nifedipine

(50 μM) on I_{to1} (+50 mV) was observed at frequencies from 1 to 3 Hz ($n=6$, $P=$NS).

Inhibition of I_{Kur} *by nifedipine*

Figure 10A illustrates the time course of I_{Kur} during control and after applying 30 μM nifedipine, and washout of the drug in a typical experiment. I_{Kur} was reversibly decreased by nifedipine. Figure 10B displays the effect of nifedipine on voltage-dependent I_{Kur} in a representative myocyte. Nifedipine at 5 and 50 μM produced a substantial suppression on I_{Kur}, and the effect was recovered by the drug washout.

Figure 11a displays the *I–V* relationships of I_{Kur} under control conditions, and after the application of 1, 5, 10, 50, and 100 μM nifedipine. I_{Kur} was inhibited by nifedipine in a concentration-dependent manner, and recovered by 95% of control after washout of the drug. The percent reduction of I_{Kur} by nifedipine at potentials from 0 to +50 mV is shown in Figure 11b. Significant inhibition of I_{Kur} was observed from the low concentration of 1 μM. I_{Kur} at +50 mV was decreased by 7.7±2.6, 25.6±4.2, 48.1±4.8, 69.9±4.3, and 75.9±4.9% at 1, 5, 10, 50, and 100 μM nifedipine, respectively ($n=8$, $P<0.05$ or 0.01). Figure 11c shows the concentration-dependent response of I_{Kur} to nifedipine. On the basis of cell-by-cell fits with Hill equation completed in seven cells, all the concentrations from 0.1 to 200 μM, IC_{50} was 8.2±0.8 μM with a Hill co-efficient of 1.2±0.1, and E_{max} was 76%. No use-dependent effect of nifedipine (10 μM) on I_{Kur} (40 mV) was observed at frequencies from 1 to 3 Hz ($n=6$, $P=$NS).

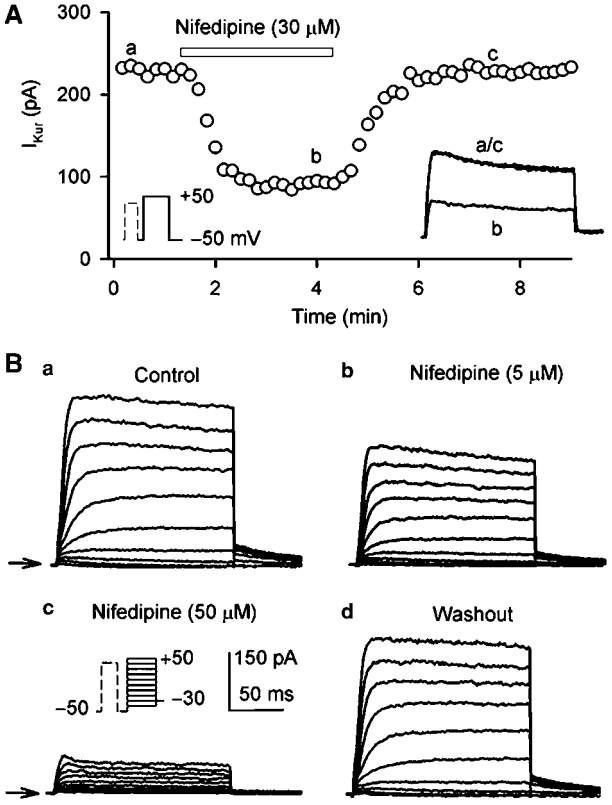

Figure 10 Effect of nifedipine on I_{Kur}. (A) Time-dependent effect of 30 μM nifedipine on I_{Kur} elicited by voltage protocol shown in the left inset delivered every 10 s in a typical experiment. Nifedipine reversibly suppressed I_{Kur}. (B) Voltage-dependent I_{Kur} recorded in a representative myocyte by the voltage protocol shown in the inset under control conditions (a), in the presence of 5 and 50 μM nifedipine for 5 min (b, c), and after wash out of the drug for 6 min (d). Nifedipine substantially suppressed I_{Kur}, and the effect recovered upon the drug washout.

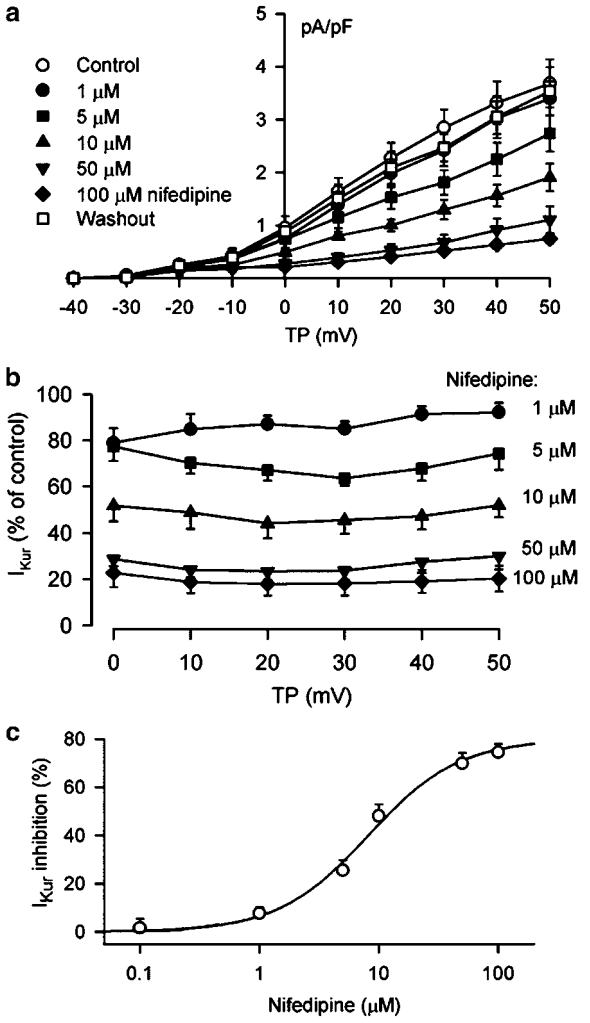

Figure 11 Nifedipine effect on voltage-dependent I_{Kur}. (a) *I–V* relationships of I_{Kur} under control conditions, in the presence of 1, 5, 10, 50, and 100 μM nifedipine (6 min for each concentration), and after the drug washout for 10 min. Nifedipine inhibited I_{Kur} in a concentration-dependent manner, and the effect was reversed by 95% (at +50 mV) by washout of the drug for 10 min. (b) Percent inhibition of I_{Kur} at voltages from 0 to +50 mV by nifedipine with multiple concentrations. Nifedipine significantly inhibited I_{Kur} at concentrations from 1 to 5, 10, 50, and 100 μM ($n=8$, $P<0.05$ or 0.01 vs control), and no voltage-dependent effect was observed for the drug action. The statistical significance was analyzed by the repeated measures ANOVA. (c) Concentration-dependent inhibition of I_{Kur} by nifedipine at +50 mV. The symbols are mean values of inhibitory effect in seven cells exposed to different concentrations of nifedipine. Solid lines were fit to Hill equation. Mean IC_{50} was 8.2±0.8 μM, Hill co-efficient was 1.2±0.2, and E_{max} was 76%.

Discussion

The present study demonstrates that the widely used Ca^{2+} channel blockers diltiazem and nifedipine substantially

inhibit the repolarization currents I_{to1} and I_{Kur} in human atrial myocytes. The blockade of human atrial I_{to1} and I_{Kur} by the two Ca^{2+} channel blockers was concentration-dependent.

The benzothiazopine Ca^{2+} channel blocker diltiazem, the dihydropyridine Ca^{2+} channel blocker nifedipine, and the phenylalkylamine Ca^{2+} channel block verapamil were reported to block a variety of cloned K^+ channels including Kv1.1, Kv1.2, Kv1.3, Kv1.4, Kv1.5, Kv3.1, Kv4.2, and HERG channel currents expressed in mammalian cell lines and/or *Xenopus* oocytes (Rampe *et al*., 1993; Grissmer *et al*., 1994; Zhang *et al*., 1997; Rolf *et al*., 2000; Calmels *et al*., 2001). Our recent study showed that verapamil inhibited I_{Kur}, but not I_{to1}, in human atrium (Gao *et al*., 2004). The present observation provides the novel information that diltiazem and nifedipine decrease both I_{to1} and I_{Kur} in human atrial myocytes.

Our findings showed that diltiazem substantially inhibited I_{to1} in human atrial myocytes, and significantly accelerated the inactivation of I_{to1}, and reduced the time to peak of the activation (Figures 1–3), suggesting an open-channel block (Feng *et al*., 1997). No report is available in literature regarding the diltiazem effect on I_{to1} to compare the results from the present observation. I_{to1} may be encoded by the cloned channel Kv1.4 or Kv4.2/Kv4.3 (Tseng, 1999). A recent report described that Kv1.4 and Kv4.2 currents expressed in *Xenopus* oocytes were inhibited by 10 and 24% at $+50$ mV with 100 μM diltiazem (Rolf *et al*., 2000). The effect is much weaker than that ($IC_{50} = 29.2\,\mu$M, $E_{max} = 65\%$) observed in human atrial native I_{to1} (Figure 3).

I_{Kur} in human atrium is generally believed to be encoded by cloned channel Kv1.5 (Fedida *et al*., 1993; Wang *et al*., 1993). It was reported that diltiazem at 100 μM blocked the cloned Kv1.5 channel currents expressed in *Xenopus* oocytes only by 15% at $+50$ mV (Rolf *et al*., 2000), and the compound inhibited the Kv1.5 channel current expressed in mouse fibroblasts with a large K_d of 115 μM (Grissmer *et al*., 1994). However, diltiazem inhibited I_{Kur} with IC_{50} of 11.2 μM in human atrial myocytes (Figures 5 and 6), suggesting that the blocking effect is stronger in human atrial native I_{Kur} than that in cloned hKv1.5 channel expressed in *Xenopus* oocytes or mouse fibroblasts (Grissmer *et al*., 1994; Rolf *et al*., 2000).

The suppression of native I_{to1} by nifedipine was initially reported in rabbit atrial cells (Gotoh *et al*., 1991), and rat ventricular myocytes (Jahnel *et al*., 1994). The present observation provides additional evidence that nifedipine also inhibits human atrial I_{to1} (Figures 7 and 8). Inactivation of I_{to1} was significantly accelerated by nifedipine in human atrial myocytes (Figure 9), suggesting an open-channel block, consistent with the reports from rabbit and rat cardiac myocytes (Gotoh *et al*., 1991; Jahnel *et al*., 1994), and cloned *Sharker* K^+ channels expressed in *Xenopus* oocytes (Avdonin *et al*., 1997).

It has been reported that human atrial I_{to1} is mainly encoded by Kv4.3 (Kong *et al*., 1998). Nifedipine had no significant effect on the kinetics of voltage-dependent activation and inactivation, and the rate of recovery from inactivation of I_{to1} in human atrial myocytes. However, nicardipine, another DHP compound, negatively shifted $V_{0.5}$ of activation and inactivation, and slowed down the rate of recovery from inactivation of rat Kv4.3L channel currents expressed in HEK 293 cell line (Hatano *et al*., 2003). These different responses of Kv4.3 to DHPs may be related to the subtle differences of the Kv4.3 sequences (human vs rat), the cell types (native human atrial cells vs HEK 293 cells), or the chemical structures (nifedipine vs nicardipine), etc.

It was reported that nifedipine substantially blocked hKv1.5 current expressed in HEK 293 cells (Zhang *et al*., 1997) and mouse fibroblast (Grissmer *et al*., 1994). The present study demonstrated that nifedipine inhibited human atrial I_{Kur} in a concentration-dependent manner, with an IC_{50} of 8.2 μM (Figures 10 and 11). The concentration is close to the K_d (6.2 μM) of hKv1.5 current expressed in HEK cells (Zhang *et al*., 1997), and lower than that of hKv1.5 current expressed in mouse fibroblasts ($K_d = 92\,\mu$M) (Grissmer *et al*., 1994). No report is available in literature from native cells to compare with the data obtained from the present observation in human atrial myocytes.

I_{Kur} is found to be functionally expressed in human atrium, but not ventricle (Li *et al*., 1996b). Therefore, the drugs that specifically inhibit the unique I_{Kur} may provide a means of preventing atrial fibrillation without the risk of ventricular proarrhythmia (Nattel, 2002). In the present study, we have found that the diltiazem inhibits I_{Kur} with an IC_{50} of 11.2 μM. The significant inhibitory effect on I_{Kur} was observed at low concentration of 1 μM, which is close to the therapeutically relevant plasma (50–300 ng ml^{-1}) concentrations of diltiazem in the treatment of atrial arrhythmias (Singh *et al*., 1983; Dias *et al*., 1992; Kelly & O'Malley, 1994), and the $I_{Ca.L}$ block concentration (1–15 μM) in myocardium (McDonald *et al*., 1994; Koidl *et al*., 1997). Nifedipine also significantly inhibited I_{Kur} at 1 μM, but the concentration is higher than the clinical relevant plasma (10–200 ng ml^{-1}) concentrations (Singh *et al*., 1983; Kelly & O'Malley, 1994), and the $I_{Ca.L}$ block concentration (0.05–0.2 μM) in myocardium (McDonald *et al*., 1994; Koidl *et al*., 1997). Whether the inhibition of I_{Kur} and I_{to1} by diltiazem or nifedipine would exert a beneficial action on supraventricular arrhythmias remains to be studied.

In summary, the present study has provided the first information that the widely used Ca^{2+} antagonists diltiazem and nifedipine substantially inhibit the repolarization currents I_{to1} and I_{Kur} in human atrial myocytes.

This work was supported by CRCG from the Research Committee of the University of Hong Kong. We thank Professor T.M. Wong in the Department of Physiology for his support.

References

AVDONIN, V., SHIBATA, E.F. & HOSHI, T. (1997). Dihydropyridine action on voltage-dependent potassium channels expressed in *Xenopus* oocytes. *J. Gen. Physiol.,* **109,** 169–180.

CALMELS, T.P., FAIVRE, J.F., CHEVAL, B., JAVRE, J.L., ROUANET, S. & BRIL, A. (2001). hKv4.3 channel characterization and regulation by calcium channel antagonists. *Biochem. Biophys. Res. Commun.,* **281,** 452–560.

COURTEMANCHE, M., RAMIREZ, R.J. & NATTEL, S. (1998). Ionic mechanisms underlying human atrial action potential properties: insights from a mathematical model. *Am. J. Physiol.,* **275,** H301–H321.

COURTEMANCHE, M., RAMIREZ, R.J. & NATTEL, S. (1999). Ionic targets for drug therapy and atrial fibrillation-induced electrical remodeling: insights from a mathematical model. *Cardiovasc. Res.,* **42,** 477–489.

DE LEEUW, P.W. & BIRKENHAGER, W.H. (2002). The effects of calcium channel blockers on cardiovascular outcomes: a review of randomised controlled trials. *Blood Press.,* **11,** 71–78.

DIAS, V.C., WEIR, S.J. & ELLENBOGEN, K.A. (1992). Pharmacokinetics and pharmacodynamics of intravenous diltiazem in patients with atrial fibrillation or atrial flutter. *Circulation,* **86,** 1421–1428.

DU, X.L., LAU, C.P., CHIU, S.W., TSE, H.F., GERLACH, U. & LI, G.R. (2003). Effects of chromanol 293B on transient outward and ultrarapid delayed rectifier potassium currents in human atrial myocytes. *J. Mol. Cell. Cardiol.,* **35,** 293–300.

FEDIDA, D., WIBLE, B., WANG, Z., FERMINI, B., FAUST, F., NATTEL, S. & BROWN, A.M. (1993). Identity of a novel delayed rectifier current from human heart with a cloned K^+ channel current. *Circ. Res.,* **73,** 210–216.

FENG, J., WANG, Z., LI, G.R. & NATTEL, S. (1997). Effects of class III antiarrhythmic drugs on transient outward and ultra-rapid delayed rectifier currents in human atrial myocytes. *J. Pharmacol. Exp. Ther.,* **281,** 384–392.

GAO, Z., LAU, C.P., CHIU, S.W. & LI, G.R. (2004). Inhibition of ultrarapid delayed rectifier K^+ current by verapamil in human atrial myocytes. *J. Mol. Cell. Cardiol.,* **36,** 257–263.

GOTOH, Y., IMAIZUMI, Y., WATANABE, M., SHIBATA, E.F., CLARK, R.B. & GILES, W.R. (1991). Inhibition of transient outward K^+ current by DHP Ca^{2+} antagonists and agonists in rabbit cardiac myocytes. *Am. J. Physiol.,* **260,** H1737–H1742.

GRISSMER, S., NGUYEN, A.N., AIYAR, J., HANSON, D.C., MATHER, R.J., GUTMAN, G.A., KARMILOWICZ, M.J., AUPERIN, D.D. & CHANDY, K.G. (1994). Pharmacological characterization of five cloned voltage-gated K^+ channels, types Kv1.1, 1.2, 1.3, 1.5, and 3.1, stably expressed in mammalian cell lines. *Mol. Pharmacol.,* **45,** 1227–1234.

HATANO, N., OHYA, S., MURAKI, K., GILES, W. & IMAIZUMI, Y. (2003). Dihydropyridine Ca^{2+} channel antagonists and agonists block Kv4.2, Kv4.3 and Kv1.4 K^+ channels expressed in HEK293 cells. *Br. J. Pharmacol.,* **139,** 533–544.

HOHNLOSER, S.H., KUCK, K.H. & LILIENTHAL, J. (2000). Rhythm or rate control in atrial fibrillation – pharmacological intervention in atrial fibrillation (PIAF): a randomised trial. *Lancet,* **356,** 1789–1794.

JAHNEL, U., KLEMM, P. & NAWRATH, H. (1994). Different mechanisms of the inhibition of the transient outward current in rat ventricular myocytes. *Naunyn-Schmiedeberg's Arch. Pharmacol.,* **349,** 87–94.

KELLY, J.G. & O'MALLEY, K. (1994). Clinical pharmakinetics of calcium antagonists. An update. *Clin. Pharmacokinet.,* **22,** 416–433.

KOIDL, B., MIYAWAKI, N. & TRITTHART, H.A. (1997). A novel benzothiazine Ca^{2+} channel antagonist, semotiadil, inhibits cardiac L-type Ca^{2+} currents. *Eur. J. Pharmacol.,* **322,** 243–247.

KONG, W., PO, S., YAMAGISHI, T., ASHEN, M.D., STETTEN, G. & TOMASELLI, G.F. (1998). Isolation and characterization of the human gene encoding I_{to}: further diversity by alternative mRNA splicing. *Am. J. Physiol.,* **275,** H1963–H1970.

KUMAR, S. & HALL, R.J. (2003). Drug treatment of stable angina pectoris in the elderly: defining the place of calcium channel antagonists. *Drugs Aging,* **20,** 805–815.

LI, G.R., FENG, J., WANG, Z., FERMINI, B. & NATTEL, S. (1995). Comparative mechanisms of 4-aminopyridine-resistant I_{to} in human and rabbit atrial myocytes. *Am. J. Physiol.,* **269,** H463–H472.

LI, G.R., FENG, J., WANG, Z., FERMINI, B. & NATTEL, S. (1996a). Adrenergic modulation of ultrarapid delayed rectifier K^+ current in human atrial myocytes. *Circ. Res.,* **78,** 903–915.

LI, G.R., FENG, J., YUE, L., CARRIER, M. & NATTEL, S. (1996b). Evidence for two components of delayed rectifier K^+ current in human ventricular myocytes. *Circ. Res.,* **78,** 689–696.

MCDONALD, T.F., PELZER, S., TRAUTWEIN, W. & PELZER, D.J. (1994). Regulation and modulation of calcium channels in cardiac, skeletal, and smooth muscle cells. *Physiol. Rev.,* **74,** 365–507.

NATTEL, S. (2002). New ideas about atrial fibrillation 50 years on. *Nature,* **415,** 219–226.

RAMPE, D., WIBLE, B., FEDIDA, D., DAGE, R.C. & BROWN, A.M. (1993). Verapamil blocks a rapidly activating delayed rectifier K^+ channel cloned from human heart. *Mol. Pharmacol.,* **44,** 642–648.

ROLF, S., HAVERKAMP, W., BORGGREFE, M., MUSSHOFF, U., ECKARDT, L., MERGENTHALER, J., SNYDERS, D.J., PONGS, O., SPECKMANN, E.J., BREITHARDT, G. & MADEJA, M. (2000). Effects of antiarrhythmic drugs on cloned cardiac voltage-gated potassium channels expressed in *Xenopus* oocytes. *Naunyn-Schmiedeberg's Arch. Pharmacol.,* **362,** 22–31.

SHIBATA, E.F., DRURY, T., REFSUM, H., ALDRETE, V. & GILES, W. (1989). Contributions of a transient outward current to repolarization in human atrium. *Am. J. Physiol.,* **257,** H1773–H1781.

SINGH, B.N., NADEMANEE, K. & BAKY, S.H. (1983). Calcium antagonists. Clinical use in the treatment of arrhythmias. *Drugs,* **25,** 125–153.

TSENG, G.N. (1999). Molecular structure of cardiac I_{to} channels: Kv4.2, Kv4.3, and other possibilities? *Cardiovasc. Res.,* **41,** 16–18.

VAN WAGONER, D.R. (2000). Pharmacologic relevance of K(+) channel remodeling in atrial fibrillation. *J. Mol. Cell. Cardiol.,* **32,** 1763–1766.

VAN WAGONER, D.R. & NERBONNE, J.M. (2000). Molecular basis of electrical remodeling in atrial fibrillation. *J. Mol. Cell. Cardiol.,* **32,** 1101–1117.

WANG, Z., FERMINI, B. & NATTEL, S. (1993). Sustained depolarization-induced outward current in human atrial myocytes. Evidence for a novel delayed rectifier K^+ current similar to Kv1.5 cloned channel currents. *Circ. Res.,* **73,** 1061–1076.

WHITE, W.B. (2003). Clinical trial experience around the globe: focus on calcium-channel blockers. *Clin. Cardiol.,* **26,** II7–II11.

ZHANG, X., ANDERSON, J.W. & FEDIDA, D. (1997). Characterization of nifedipine block of the human heart delayed rectifier, hKv1.5. *J. Pharmacol. Exp. Ther.,* **281,** 1247–1256.

(Received September 23, 2004
Revised October 25, 2004
Accepted November 23, 2004)